HemaSphere
Powered by EHA

EHA EUROPEAN HEMATOLOGY ASSOCIATION

Article
OPEN ACCESS

The Complexity of Genotype-Phenotype Correlations in Hereditary Spherocytosis: A Cohort of 95 Patients

Genotype-Phenotype Correlation in Hereditary Spherocytosis

Annelies van Vuren[1], Bert van der Zwaag[2], Rick Huisjes[3], Nathalie Lak[4], Marc Bierings[5], Egbert Gerritsen[6], Eduard van Beers[7], Marije Bartels[8], Richard van Wijk[9]

Correspondence: Richard van Wijk (e-mail: R.vanWijk@umcutrecht.nl).

Abstract

Hereditary spherocytosis (HS) is a phenotypically and genetically heterogeneous disease. With the increased use of Next Generation Sequencing (NGS) techniques in the diagnosis of red blood cell disorders, the list of unique pathogenic mutations underlying HS is growing rapidly. In this study, we aimed to explore genotype-phenotype correlation in 95 HS patients genotyped by targeted NGS as part of routine diagnostics (UMC Utrecht, Utrecht, The Netherlands). In 85/95 (89%) of patients a pathogenic mutation was identified, including 56 novel mutations. *SPTA1* mutations were most frequently encountered (36%, 31/85 patients), primarily in patients with autosomal recessive forms of HS. Three *SPTA1* (α-spectrin) mutations showed autosomal dominant inheritance. *ANK1* (ankyrin1) mutations accounted for 27% (23/85 patients) and *SPTB* (β-spectrin) mutations for 20% (17/85 patients). Moderate or severe HS was more frequent in patients with *SPTB* or *ANK1* mutations, reflected by lower hemoglobin concentrations and higher reticulocyte counts. Interestingly, mutations affecting spectrin association domains of *ANK1*, *SPTA1* and *SPTB* resulted in more severe phenotypes. Additionally, we observed a clear association between phenotype and aspects of red cell deformability as determined by the Laser assisted Optical Rotational Cell Analyzer (LoRRca MaxSis). Both maximal deformability and area under the curve were negatively associated with disease severity (respectively $r=-0.46$, $p<0.01$, and $r=-0.39$, $p=0.01$). Genotype-phenotype prediction in HS facilitates insight in consequences of pathogenic mutations for the assembly and dynamic interactions of the red cell cytoskeleton. In addition, we show that measurements of red blood cell deformability are clearly correlated with HS severity.

Author Contributions: MBi, EG, EB, MBa and RW were directly or indirectly involved in the care of patients and/or diagnostics. AV analyzed and interpreted the data, wrote the manuscript. RW and BZ contributed to the analysis; EB, MBa, BZ and RW contributed to the writing of the manuscript. All authors listed have made a substantial, direct and intellectual contribution, and approved it for publication.

RvW and EJvB are scientific advisors to RR Mechatronics and their research is in part funded by an unrestricted grant provided by RR Mechatronics.

The other authors declare that the research was conducted in the absence of any commercial or financial relationships that could be construed as a potential conflict of interest.

Supplemental Digital Content is available for this article.

[1]Van Creveldkliniek, Department of Internal Medicine, University Medical Center Utrecht, Utrecht University, Utrecht, The Netherlands
[2]Department of Genetics, University Medical Center Utrecht, Utrecht University, Utrecht, The Netherlands
[3]Department of Clinical Chemistry and Haematology, University Medical Center Utrecht, Utrecht University, Utrecht, The Netherlands
[4]Princess Maxima Center for Pediatric Oncology, Wilhelmina Children's Hospital, University Medical Center Utrecht, Utrecht, The Netherlands
[5]Department of Stem cell transplantation, Princess Maxima Centre for Paediatric Oncology, Wilhelmina Children's Hospital, University Medical Center Utrecht, Utrecht, The Netherlands
[6]Department of Pediatrics, ADRZ Medical Center, Goes, The Netherlands
[7]Van Creveldkliniek, Department of Internal Medicine, University Medical Center Utrecht, Utrecht University, Utrecht, The Netherlands
[8]Pediatric Hematology, University Medical Center Utrecht, Utrecht University, Utrecht, The Netherlands
[9]Department of Clinical Chemistry and Haematology, University Medical Center Utrecht, Utrecht University, Utrecht, The Netherlands.

Copyright © 2019 the Author(s). Published by Wolters Kluwer Health, Inc. on behalf of the European Hematology Association. This is an open access article distributed under the terms of the Creative Commons Attribution-NonCommercial-ShareAlike 4.0 License, which allows others to remix, tweak, and build upon the work non-commercially, as long as the author is credited and the new creations are licensed under the identical terms.

HemaSphere (2019) 3:4(e276)

Received: 8 March 2019 / Received in final form: 20 May 2019 / Accepted: 26 May 2019

Citation: van Vuren A, van der Zwaag B, Huisjes R, Lak N, Bierings M, Gerritsen E, van Beers E, Bartels M, van Wijk R. The Complexity of Genotype-Phenotype Correlations in Hereditary Spherocytosis: a Cohort of 95 Patients. *HemaSphere*, 2019;3:4. http://dx.doi.org/10.1097/HS9.0000000000000276

Introduction

Hereditary spherocytosis (HS) is the most common inherited hemolytic anemia in individuals from North Europe and North America, affecting approximately 1:2000 individuals.[1,2] HS is genetically and phenotypically highly heterogeneous. The disease is characterized by altered red blood cell (RBC) membrane integrity due to mutations in genes encoding membrane or cytoskeletal proteins.[1] The RBC membrane is composed of approximately 20 major proteins and at least 850 minor proteins with differential expression and functionality, including transport proteins, adhesion proteins and signaling receptors.[2,3] The integral membrane proteins are organized into macromolecular complexes centered on band 3. The main components of the cytoskeleton are spectrin, actin, and its associated proteins, protein 4.1R and ankyrin.[3] Together, these proteins provide the RBC membrane with a high degree of flexibility and elasticity, allowing the cell to deform with linear extensions up to 250%.[1,4] The common hallmark of RBC in HS is disruption of the vertical association between the cytoskeleton and the overlying lipid bilayer.[5,6] HS mutations lead to reduced expression or impaired incorporation of one of the major proteins of the cytoskeleton or membrane, resulting in an imbalance in spatial protein configuration. The degree of imbalance depends on compensation by normal alleles in single heterozygotes, or by other mutations in compound heterozygotes.[7] Ultimately, destabilization of the lipid bilayer leads to loss of membrane lipids, and, therefore, loss of surface area.[8] This results in RBCs that become progressively spheroidal with reduced deformability, impeding traversing the narrow apertures of the splenic vascular walls. Spherocytes will be sequestered in the spleen leading to premature removal of RBCs.[9] The severity of HS is directly related to the extent of loss of surface area, and consequently the degree of spherocytosis: among the red cell indices the percentage of microcytes was the best indicator of disease severity.[10–12] While knowledge on the static structure of the RBC cytoskeleton markedly increased over the last decades, insights in the dynamic capacities, and the impact of genetic defects on the function of membrane proteins remain limited.[3]

HS is based on the pathophysiological effects of defects in genes encoding for one or more of the major RBC cytoskeleton and (trans)membrane proteins: ankyrin-1 (*ANK1*), band-3 (*SLC4A1*), α-spectrin (*SPTA1*), β-spectrin (*SPTB*) and protein 4.2 (*EPB42*).[6,13] We have previously demonstrated that using targeted NGS, a probable causative mutation (and 29 unique mutations) could be identified in these genes in 85% of HS patients (27/33).[14] Compared to Sanger sequencing, targeted-next-generation sequencing (NGS) of preselected gene panels has a higher diagnostic efficiency and, thereby, rapidly provides a thorough genetic analysis in patients suspected of RBC membrane disorders.[13,15,16] Currently, making the diagnosis of HS is multi-facetted: reports of clinical and family history, analysis of biochemical hemolysis parameters, analysis of RBC morphological features, and functional testing, including the osmotic fragility test, eosin-5-maleimide (EMA) binding test[17] and, more recently, osmotic gradient ektacytometry.[18,19] Overall, in 75% of the HS patients, there is an autosomal dominant (AD) inheritance pattern, whereas in the remaining 25% of patients HS is inherited in an autosomal recessive (AR) way, or is due to a de novo mutation.[6] Originally, in Northern Europe and the USA, *ANK1* mutations were shown to account for 40% to 65% of the cases, *SLC4A1* mutations for 20% to 35%, *SPTB1* mutations for 15% to 30%, and *SPTA1* and *EPB42* each for less than 5% of the HS cases.[6,20] Interestingly, in Japan, mutations in *EPB42* (45–50%) and *SLC4A1* (20–30%) were most abundant.[6,21]

More than 10 years ago Iolascon and Avvisati already hypothesized on the existence of genotype/phenotype correlations in hereditary spherocytosis by stating that the biochemical and genetic heterogeneity of spherocytosis could represent the basis for clinical heterogeneity.[22] With the growing list of, mostly unique, HS mutations, attempts have been made to unravel the relationship between genotype and phenotype.[13,23–25] Mild, moderate, and severe forms of HS have been defined according to severity of anemia and degree of compensation for hemolysis. (Table S1, http://links.lww.com/HS/A41)[5,6,9,26,27] From these studies, AR forms of HS due to mutations in the *SPTA1* gene combining low expression and null alleles seemed to be associated with a more severe phenotype. Among the mutations in other HS genes, there was a broad variability in phenotypic presentation.[13,23–25] So, until now, a clear genotype-phenotype correlation in HS has not been observed.

Here, we present a large cohort consisting of 95 HS patients in whom 56 novel pathogenic mutations, including 3 apparently AD *SPTA1* mutations, were identified. Our data provide novel insights in the highly complex genotype-phenotype correlation in HS due to the complexity of the interactions in the RBC cytoskeleton. Based on our findings, we conclude that knowledge of underlying molecular defects, as well as functional analysis of RBC deformability, is required to understand phenotypic variability in HS. Future studies exploring the direct effects of genetic mutations on RBC protein expression and function will be necessary to further elucidate genotype-phenotype correlations.

Results

Overview mutations and disease severity

Our cohort included 95 patients suspected to have HS. Clinical characteristics and median laboratory parameters are provided in Table 1. Cholecystectomy and splenectomy were simultaneously performed in 6/11 patients who underwent splenectomy in the last 10 years. Table 2 shows the identified HS mutations categorized per gene, including the pathogenicity classification for the novel mutations (according to recommendations for interpretation)[28] and phenotype per patient. In 85 patients, a mutation was identified in one of the HS associated genes, 56 new pathogenic HS mutations were reported. Three disease-causing mutations were identified in 2 (*SPTA1* c.5791C>T p.(Gln2931); and *SLC4A1* c.37G>T p.(Glu13*)) or 3 (*SPTA1* c.83G>A p.(Arg28His)) seemingly unrelated families.

SPTA1 mutations were identified in 31/85 (36.5%) of the HS cases in our cohort, *ANK1* in 23/85 (27.1%), *SPTB* in 17/85 (20.0%), *SLC4A1* in 13/85 (15.2%) and *EPB42* in 1/85 (1.2%) patients (Fig. 1A). In 10/95 (10.5%) of the patients no mutation could be identified. Missense mutations accounted for 23/85 (24.2%) of the identified mutations, the remaining mutations were nonsense, frameshift, indels or splice site mutations. In 65/95 patients (68.4%) HS was inherited in an apparent AD manner, AR inheritance was reported in 23/95 (24.2%) patients. In the remaining number of 7/95 (7.4%) patients, the inheritance mode could not be identified. Interestingly, all mutations in *ANK1*, *SLC4A1*, *SPTB*, and *EPB42* showed an AD inheritance pattern, except one *SPTB* mutation in which the inheritance pattern was unknown.

Table 1

Patient Characteristics.

	Without or before splenectomy	Post-splenectomy
Number of patients (N)	70	19
Age (years) – genetic analysis	30 (22)	28 (19)
Gender (% male)	49	47
Laboratory parameters [reference range]		
Hb (g/dL) [11.9–17.2]	11.6 (2.4)	14.2 (1.8)
MCV (fL) [80–97]	87 (9)	87 (9)
MCH (fmol) [1.75–2.25]	1.9 (0.2)	1.9 (0.2)
MCHC (mmol/L) [19–23]	21.9 (0.9)	21.6 (0.8)
Reticulocyte count. absolute (x10^9/L) [25–120]	381 (220)	222 (160)
Platelets (x10^9/L) [150–450]	243 (112)	486 (215)
Leukocytes (x10^9/L) [4–10]	7.4 (2.7)	9.4 (1.7)
LD (U/L) [0–250]	297 (199)	224 (60)
Bilirubin (μmol/L) [3–21]	48 (34)	21 (12)
AST (U/L) [0–35]	29 (11)	36 (15)
Ferritin (μg/L) [20–250]	339 (500)	129 (95)
HS diagnotics		
EMA (%)	78 (12)	75 (9)

The 82 of the 95 included patients had hematological data available. Of 7 patients data obtained before and after splenectomy were available. Mean values are presented (±Standard Deviation). EMA = eosin-5-maleimide binding test.

We investigated the correlation between affected gene and disease severity, hematologic parameters, and EMA test results. The fraction of patients with moderate or severe phenotypes was highest among patients with *SPTB* (12/15, 80%) and *ANK1* mutations (13/19, 68.4%) (Fig. 1B). Hemoglobin levels were available for 62 non-splenectomized patients (or obtained from patients before splenectomy) with an identified mutation, all values obtained post-splenectomy were excluded (Table 3). Five of the 6 patients with phenotypically severe HS and who not underwent splenectomy required regular red cell transfusions. Mean hemoglobin levels were significantly lower in in HS patients with *SPTB* mutations, compared to patients with *SCL4A1* mutations ($p = 0.05$), and in patients with *ANK1* mutations compared to patients with *SLC4A1* mutations ($p = 0.04$). In agreement with mean hemoglobin levels, absolute reticulocyte counts, in patients without splenectomy or obtained before splenectomy, differed significantly between patients from genetic subgroups. Reticulocyte counts were significantly higher in patients with *ANK1* mutations than in patients with *SCL4A1* ($p < 0.01$) and *SPTA1* mutations ($p < 0.01$); and in patients with *SPTB* mutations compared to patients with *SCL4A1* ($p < 0.01$) and *SPTA1* mutations ($p = 0.02$). Bilirubin, lactate dehydrogenase, and aspartate aminotransferase concentrations did not differ statistically between the genetic subgroups. EMA values, available in 42 patients without or obtained before splenectomy, were significantly higher in HS patients with *SPTA1* mutations compared to patients with *ANK1* ($p < 0.01$), *SPTB* ($p < 0.01$) and *SLC4A1* ($p = 0.04$) mutations.

Mutations in the spectrin-binding domains of ANK1, SPTA1 and SPTB are associated with a more severe HS phenotype.

Next, we investigated the correlation between clinical phenotype and genetic mutations using protein structure information. Pathogenic mutations were mapped along the protein structures of ankyrin-1, α-spectrin, β-spectrin and band 3 (overview depicted in Fig. 2A–D). All mutations in the *ANK1* gene followed an AD inheritance pattern. Six of the identified mutations were positioned in the spectrin-binding domain of *ANK1*: 5/6 of these mutations resulted in a moderate or severe phenotype. Remarkably, mutations closely positioned to each other (eg, *ANK1* c.841C>T p.(Arg281*) and c.856C>T p.(Arg286*), as well as *ANK1* c.341C>T p.(Pro114Leu) and c.344T>C p.(Leu115Pro)) resulted in completely different HS phenotypes. Intriguingly, 3 novel pathogenic mutations in *SPTA1* were detected that apparently were inherited in an AD fashion. Disease severity varied in these patients from mild to severe. In our cohort, the majority of patients with autosomal recessive *SPTA1* mutations had a mild phenotype (11/19). Notably, 2 mutations in repeat 21 of *SPTA1*, the binding domain for β-spectrin, and a mutation in the α-spectrin-binding domain of *SPTB* resulted in a (more) severe phenotype. Interestingly, a large deletion, including the whole *SPTB* gene (*SPTB* c.1-?_6414+?del), resulted in a mild phenotype, while the majority of other pathogenic mutations in the *SPTB* gene were associated with a more severe disease phenotype, suggesting that incorporation of a truncated protein might be occurring and be more harmful than an absolute decrease of otherwise normal protein. Pathogenic *SCL4A1* mutations resulted in a mild phenotype in 9/11 patients. None of the pathogenic mutations involved one of the known binding sites of band 3 with other cytoskeleton proteins. In summary, our data showed that patients with a mutation in the domains for spectrin dimer-tetramer association (*SPTA1* and *SPTB*) and ankyrin-spectrin-binding (*ANK1*) show a more severe disease phenotype compared to patients with other pathogenic HS mutations. No other clear patterns between mutations in specific domains and phenotypes could be identified.

Phenotypic variability of HS exists within families

In order to further study genotype-phenotype correlation, we evaluated the phenotypic expression of HS within families harboring the same HS-causing mutation. Our cohort included 9 such families, of which clinical data was available from all family members in 7 families. Phenotypic expression of HS was roughly similar among members of 3 families (family A, F, H in Table 3). However, more broad phenotypic variability was observed in 4 other families, despite identical genotypes among individual family members (family B, D, G, I). This phenotypic heterogeneity was particularly evident in family G and I (Fig. 3).

In family G, dizygotic twins shared the same pathogenic *ANK1* mutation. In patient I the mutation resulted in a moderate phenotype with mild anemia, reticulocytosis and splenomegaly. In patient II the mutation resulted in a severe phenotype requiring splenectomy at the age of 13 years. Phenotypical variation could not be explained by other (modifying) mutations in the analyzed genes.

Table 2

Pathogenic Mutations in the HS cohort. List of Individual Patients, Apparent Inheritance Pattern, Identified Mutations, and Disease Phenotype.

No	Family	Type mutation	Inheritence pattern	Gene	Allele 1	Pathogenicity 1	Allele 2	Pathogenicity 2	LELY[a]	Phenotype
1	A	missense	AR	SPTA1	c.83G>A p.(Arg28His)	5-P			heterozygous	Severe
2	A	missense	AR	SPTA1	c.83G>A p.(Arg28His)	5-P			heterozygous	Moderate
3		missense	AR	SPTA1	c.83G>A p.(Arg28His)	5-P			heterozygous	Severe
4		missense	AR	SPTA1	c.83G>A p.(Arg28His)	5-P			heterozygous	Severe
5		missense	AR	SPTA1	c.101G>C p.(Arg34Pro)	5-P			heterozygous	Mild
				SLC4A1	c.1162C>T p.(Arg388Cys)	3-VUS				
6		other	AR	SPTA1	c.678G>A p.(Glu227Valfs*10)[#]	5-P			homozygous	Mild
7		other	AR	SPTA1	c.1273C>T p.(Arg425*)	5-P			normal	Mild
8	B	other	AD	SPTA1	c.1850dup p.(Ser618Glufs*10)	5-P			normal	Moderate
9	B	other	AD	SPTA1	c.1850dup p.(Ser618Glufs*10)	5-P			normal	Mild
10	B	other	AD	SPTA1	c.1850dup p.(Ser618Glufs*10)	5-P			normal	Mild
11	B	other	AD	SPTA1	c.1850dup p.(Ser618Glufs*10)	5-P			heterozygous	Mild
12		other	AD	SPTA1	c.1959T>A p.(Tyr653*)	5-P			normal	Mild
13		other	AR	SPTA1	c.2353C>T p.(Arg785*)	5-P			heterozygous	Moderate
14		other	AR	SPTA1	c.2755G>T p.(Glu919*)	5-P			heterozygous	Mild
15		other	AR	SPTA1	c.2806–13T>G p.(?)	5-P	c.4339–99C>T p.(?)[b]	5-P	normal	Mild
				SLC4A1	c.118G>A p.(Glu40Lys)	3-VUS				
16		other	AR	SPTA1	c.3257dup p.(Leu1086Phefs*5)	5-P			heterozygous	Moderate
17		other	unknown	SPTA1	c.3569+2T>C p.(?)	5-P			homozygous	Mild
18		other	unknown	SPTA1	c.4081del p.(His1361Metfs*15)	5-P			heterozygous	Mild
19		missense	AD	SPTA1	c.4240C>T p.(Arg1414Cys)	4-LP			normal	Severe
20		other	AR	SPTA1	c.4339–99C>T p.(?)[b]	5-P	c.6769G>T (p.Glu2257*)	5-P	normal	Moderate
21		other	AR	SPTA1	c.4339–99C>T p.(?)[b]	5-P	c.4339–99C>T p.(?)[b]	5-P	normal	Mild
22		other	AR	SPTA1	c.4339–99C>T p.(?)[b]	5-P	c.4339–99C>T p.(?)[b]	5-P	normal	Mild
23		other	AR	SPTA1	c.4339–99C>T p.(?)[b]	5-P	c.4339–99C>T p.(?)[b]	5-P	normal	Mild
24		other	AR	SPTA1	c.5941C>T p.(Gln1981*)[##]	5-P	c.[4339–99C>T[b];4347G>T] p.[(?);(Lys1449Asn)]	5-P; 3-VUS	normal	Mild
25		other	unknown	SPTA1	c.4339–99C>T p.(?)[b]	5-P			normal	Mild
26		other	unknown	SPTA1	c.4339–99C>T p.(?)[b]	5-P			normal	Mild
				SLC4A1	c.2494C>T p.(Arg832Cys)	3-VUS				
27		other	unknown	SPTA1	c.4738–1G>A p.(?)	5-P			normal	Moderate
28		other	AR	SPTA1	c.5791C>T p.(Gln1931*)	5-P			homozygous	Mild
29		other	AR	SPTA1	c.5791C>T p.(Gln1931*)	5-P			homozygous	Mild
30		other	AR	SPTA1	c.5941C>T, p.(Gln1981*)	5-P	c.[4339–99C>T;c.4347G>T] p.[(?);(Lys1449Asn)]	5-P; 3-VUS	normal	
31		other	AR	SPTA1	c.6843–2A>G	5-P	c.6843–2A>G p.(?)	5-P	normal	Moderate
32	C	missense	AD	ANK1	c.245T>C p.(Leu82Pro)	4-LP				
33	C	missense	AD	ANK1	c.245T>C p.(Leu82Pro)	4-LP				
34		missense	AD	ANK1	c.341C>T p.(Pro114Leu)	4-LP			homozygous	Severe
35	D	missense	AD	ANK1	c.344T>C p.(Leu115Pro)	4-LP				Mild
36	D	missense	AD	ANK1	c.344T>C p.(Leu115Pro)	4-LP			heterozygous	Moderate
37		other	AD	ANK1	c.498C>G p.(Tyr166*)	5-P				Moderate
38		other	AD	ANK1	c.841C>T p.(Arg281*)	5-P				Severe
39		other	AD	ANK1	c.856C>T p.(Arg286*)	5-P				Mild
40	E	missense	AD	ANK1	c.971T>C p.(Leu324Pro)	5-P				
41	E	missense	AD	ANK1	c.971T>C p.(Leu324Pro)	5-P				Mild
42		other	AD	ANK1	c.1306–8T>G p.(?)	3-VUS				Mild
43		other	AD	ANK1	c.2559–2A>G	5-P				Moderate
44		other	AD	ANK1	c.2625del p.(Glu876Serfs*40)	5-P			heterozygous	Moderate
45		other	AD	ANK1	c.3649_3650insT p.(Pro1217Leufs*5)	5-P				Severe
46		other	AD	ANK1	c.3754C>T p.(Arg1252*)	5-P			homozygous	Severe
47		other	AD	ANK1	c.3985G>T p.(Val1329Leu)[$]	4-LP			heterozygous	Mild
48		other	AD	ANK1	c.4105–1G>A p.(?)	5-P				Severe
49		other	AD	ANK1	c.5005G>T p.(Glu1669*)	5-P				
50	F	other	AD	ANK1	c.5044C>T, p.(Arg1682*)	5-P			normal	Moderate
51	F	other	AD	ANK1	c.5044C>T, p.(Arg1682*)	5-P			heterozygous	Severe
52		other	AD	ANK1	c.5079_5080insTCAG p.(Glu1694Serfs*48)	5-P				Mild
53	G	other	AD	ANK1	c.5201_5202insTCAG p.(Thr1735Glnfs*7)	5-P				Severe
54	G	other	AD	ANK1	c.5201_5202insTCAG p.(Thr1735Glnfs*7)	5-P				Moderate
55		other	AD	SLC4A1	c.37G>T p.(Glu13*)	5-P				Mild
56		other	AD	SLC4A1	c.37G>T p.(Glu13*)	5-P				Mild
57		other	AD	SLC4A1	c.577_578del p.(Ser193Leufs*9)	5-P				Mild
58		other	AD	SLC4A1	c.620del p.(Gly207Alafs*24)	5-P				Moderate
59		other	AD	SLC4A1	c.787del p.(Arg263Alafs*34)	5-P				Mild
60		missense	AD	SLC4A1	c.1421C>A p.(Ala474Asp)	4-LP				Mild
61		other	AD	SLC4A1	c.1430C>A p.(Ser477*)	5-P				Mild
62		missense	AD	SLC4A1	c.1462G>A p.(Val488Met)	5-P				Severe
63	H	other	AD	SLC4A1	c.2057+1G>A p.(?)	5-P				Mild
64	H	other	AD	SLC4A1	c.2057+1G>A p.(?)	5-P				Mild
65		missense	AD	SLC4A1	c.2138G>T p.(Gly713Val)	4-LP				
66		missense	AD	SLC4A1	c.2348T>A p.(Ile783Asn)	5-P				Mild
67		missense	AD	SLC4A1	c.2423G>A p.(Arg808His)	5-P				Moderate
68		other	AD	SPTB	c.1-?_6414+?del p.(?)[$$]	5-P			heterozygous	Mild
69		other	unknown	SPTB	c.648-?_4002+?dup p.(?)[¥]	5-P			normal	
				SPTA1	c.2373C>A p.(Asp791Glu)	5-P				
				EPB41	c.225T>G p.(Phe75Leu)	3-VUS				
70		missense	AD	SPTB	c.544T>G p.(Trp182Gly)	5-P				Severe

(*continued*)

Table 2
(continued).

No	Family	Type mutation	Inheritence pattern	Gene	Allele 1	Pathogenicity 1	Allele 2	Pathogenicity 2	LELY[a]	Phenotype
				SLC4A1	c.118G>A p.(Glu40Gly)	3-VUS				
71		missense	AD	SPTB	c.647G>A p.(Arg216Gln)	4-LP				Moderate
72		other	AD	SPTB	c.1069C>T p.(Gln357*)	5-P			homozygous	Severe
73		other	AD	SPTB	c.1540C>T p.(Gln514*)	5-P				
74		other	AD	SPTB	c.1912C>T p.(Arg638*)	5-P				Moderate
75		other	AD	SPTB	c.2136_2137delinsTT p.(Gln713*)	5-P				Moderate
76		other	AD	SPTB	c.2137C>T p.(Gln713*)	5-P			heterozygous	Moderate
77	I	other	AD	SPTB	c.3449G>A p.(Trp1150*)	5-P			homozygous	Severe
78	I	other	AD	SPTB	c.3449G>A p.(Trp1150*)	5-P			homozygous	Severe
79	I	other	AD	SPTB	c.3449G>A p.(Trp1150*)	5-P			homozygous	Moderate
80	I	other	AD	SPTB	c.3449G>A p.(Trp1150*)	5-P				Severe
81		other	AD	SPTB	c.3581del p.(Leu1194Trpfs*32)	5-P			normal	Severe
				SPTA1	c.4339–99C>T p.(?)[b]	5-P				
82		other	AD	SPTB	c.4267C>T p.(Arg1423*)	5-P				Mild
83		other	AD	SPTB	c.4542dup p.(Leu1515Thrfs*12)	5-P			normal	Moderate
				SPTA1	c.3565C>T, p.(His1189Tyr)	3-VUS				
84		missense	AD	SPTB	c.6203T>G p.(Leu2068Arg)	4-LP				Mild
85		missense	AD	EPB42	c.554G>C p.(Arg185Pro)	4-LP				Mild
86			AR	NONE						Moderate
87			AR	NONE						Moderate
88			AR	NONE						Mild
89			unknown	NONE						Moderate
90			unknown	NONE						Mild
91			AD	NONE						
92			AD	NONE						Moderate
93			AD	NONE						Mild
94			AD	NONE						Mild
95			AD	NONE						

Families are depicted with a letter. Mutation nomenclature is according to the HGVS variation nomenclature guidelines[53] and based on the following NCBI Reference Sequence transcriptnumbers *SPTA1: NM_003126.3; SPTB: NM_000347.5; SLC4A1: NM_000342.3; ANK1: NM_000037.3; RHAG: NM_000324.2; EPB41: NM_004437.3; and EPB42: NM_000119.2.* The presence of an α^{LELY} status was reported in all patients with a SPTA1 mutation, and in other patients if known. Sequence variants were interpreted according to the recommendations of the American College of Medical Genetics and Genomics using standard terminology to describe identified variants: 1-B Benign, 2-LB Likely Benign, 3-VUS Variance of Unknown Significance, 4-LP Likely Pathogenic, 5-P Pathogenic.[28].

[a] α^{LELY} mutation: low expression allele LYON. Composed of 2 *in cis* variants in *SPTA1:* c.[5572C>G;c.6531–12C>T] p.[(Leu1858Val);(?)] ultimately resulting in strongly reduced amounts of α-spectrin. Allele frequency in the European population 29% (http://gnomad.broadinstitute.org/variant/1-158597507-G-C), not associated with hemolysis on its own.[16,54].

[b] α^{LEPRA} mutation: low expression allele PRAGUE. c.4339-99C>T mutation in the *SPTA1* gene. The mutation enhances an alternative acceptor splice site, frameshift and ultimately premature termination of translation. Approximately 1/6 of the transcripts escapes alternative splicing, resulting in low α-spectrin production. Accounts for nearly 5% of SPTA1 alleles among white people.[16,36].

[#] The *SPTA1* c.678G>A p.(Glu227Valfs*10) mutation, tested on RNA level, resulted in a 5 base pair intron retention (r.678_678+1insGUGAG) and was subsequently identified as a frameshift mutation.

[##] De novo stop-gain mutation in index patient. DNA analysis was performed in both parents.

[$] De novo mutation in index patient. DNA analysis was performed in both parents. The *ANK1* c.3985G>T p.(Val1329Leu) mutation results in alteration of the first nucleotide of exon 35 of *ANK1*. This alteration might negatively influence splicing of pre-mRNA, resulting in disturbed maturation of the *ANK1* transcript. Although, experimental evidence supporting this suggestion currently lacks.

[$$] The *SPTB* c.1-?_6414+?del p.(?) mutation results in deletion of the whole *SPTB* gene.

[¥] The *SPTB* c.648-?_4002+?dup p.(?) mutation results in duplication of exons 6-18 of the SPTB gene.

In family I, both the father and his 3 children shared the same pathogenic *SPTB* mutation. All 3 were also homozygous for the α-LELY mutation (data not shown). Father, sibling I and III had a comparable severe phenotype, including regular transfusion requirements before splenectomy. Surprisingly, sibling II however had a milder phenotype and has thus far never been transfused. Notably, her Osmoscan curve was more right-shifted (increased Ohyper) compared to the other family members carrying the identical pathogenic *SPTB* mutation.

Osmoscan parameters significantly correlate with clinical severity of HS

To further understand pathophysiological mechanisms underlying HS phenotypes and to identify alternative predictors of clinical severity we analyzed RBC osmotic deformability profiles. RBC Osmoscan profiles and information on disease severity were available for 53 patients. Nine Osmoscan profiles were obtained post-splenectomy and therefore excluded from the analysis (Fig. 4A–D). The analysis included 28 patients with phenotypically mild, 12 patients with moderate and 4 patients with severe spherocytosis. Each of the 4 patients with severe spherocytosis harbored a unique mutation in *SPTB* (3 patients) or *ANK1* (1 patient). The Area Under the Curve (AUC) was below the reference limit in all patients diagnosed with HS; 43/44 patients had an EImax value (maximum Elongation Index) below the reference range; 25/44 patients had an Ohyper value (reflecting cellular hydration status) below the reference limit; and 23/44 had an Omin value (osmotic value where EI is minimal) above the reference range.

In all patients, independent of disease severity, there was a strong correlation between EImax and AUC ($r=0.88$, $p<0.01$). EImax and AUC were both clearly, negatively associated with Omin values (respectively $r=-0.49$, $p<0.01$, and $r=-0.40$, $p<0.01$), in the absence of a clear correlation with Ohyper values. Interestingly, even in this small subset of our cohort, both EImax and AUC were clearly negatively associated with disease severity (respectively $r=-0.46$, $p<0.01$, and $r=-0.39$, $p=0.01$). Additionally, there was a positive correlation between Omin and disease severity ($r=0.31$, $p=0.04$). Furthermore, in this subgroup EMA results were also associated with disease severity ($r=-0.36$, $p=0.03$).

EImax values were significantly higher in mild (0.55) compared to moderate phenotypes (0.51) (mean difference 0.04, 95% CI [0.01; 0.07]). The mean AUC was significantly lower in patients with mild phenotypes (129) compared to patients with severe phenotypes (116) (mean difference 13, 95% CI [4; 20]). Mean Omin values were minimal, although significantly, lower in

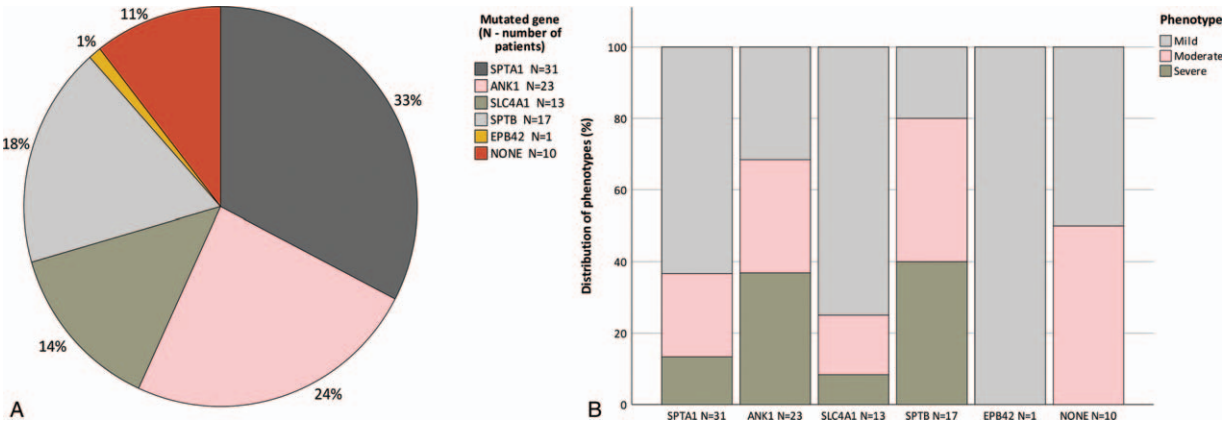

Figure 1. Overview of mutated genes and phenotype. The cohort included a total number of 95 patients diagnosed with HS. Patients were categorized according to gene with the HS mutation. A graphic overview of the distribution of the cohort is provided in *Panel A*. *Panel B* shows the distribution of HS phenotypes per gene category. N is number of patients.

patients with mild (173) compared to patients with severe HS (189) (mean difference 16, 95% CI [1; 33]). No statistical differences in Ohyper values were observed between patients with distinct HS severity.

In summary, our data shows that clinical disease severity in HS is clearly associated with 3 read out parameters of the Osmoscan profile: EImax, AUC and Omin.

Discussion

We studied the genotype-phenotype correlation in a unique, large cohort of HS patients utilizing targeted-NGS-based gene analysis of *SPTA1, SPTB, ANK1, EPB41, EPB42, SLC4A1,* and *RHAG*. Pathogenic mutations were identified in 85/95 patients. As a result, 56 novel mutations were added to the currently known HS mutations. Intriguingly, we identified 3 novel pathogenic *SPTA1* mutations that were apparently inherited in an AD fashion. We showed that overall patients with *ANK1* and *SPTB* mutations, and especially patients with *ANK1*, *SPTB* and *SPTA1* mutations in the spectrin-binding domains, were more severely affected. Furthermore, we demonstrated that EImax, AUC and Omin, the diagnostically most important parameters of RBC deformability in the Osmoscan, can be used as markers of disease severity.

While mutations in *SPTB* and *ANK1* were associated with more severe phenotypes in our cohort, we conclude that categorization in genetic subgroups (*ANK1, SPTA1, SPTB, SCL4A1, or EPB42*) is insufficient to precisely predict HS phenotype in our cohort: there was a broad phenotypic variability among patients in each genetic subgroup. To further increase our understanding of genotype-phenotype correlations in HS, insight in the direct effects of mutations on the assembly of the cytoskeleton and its dynamic interactions is required.[3] Previously, it has been demonstrated that some of the interactions in the ankyrin complex of the cytoskeleton are critical: disruptions of these interactions by specific mutations result in more severe disruption of cytoskeleton assembly or functioning and thereby lead to a more severe phenotype.[29] In line with this, we observed in our cohort more severe phenotypes in patients

Table 3

Erythropoietic and Hemolytic Parameters per Gene Group.

	SPTA1 N=26	ANK1 N=15	SPTB N=9	SLC4A1 N=11	EPB42 N=1
Gender (% male)	46	40	56	64	0
Laboratory parameters					
[reference range]					
Hb (g/dL) [11.9–17.2]	11.7 (2.3)	10.8 (2.2)	10.5 (2.7)	13.2 (1.9)	14.5 (-)
Reticulocyte count. absolute (x10^9/L) [25–120]	298 (185)	506 (203)	580 (214)	259 (84)	210 (-)
LD (U/L) [0–250]	274 (119)	291 (52)	495 (497)	214 (34)	247 (-)
Bilirubin (μmol/L) [3–21]	52 (53)	50 (17)	47 (20)	39 (14)	11 (-)
AST (U/L) [0–35]	33 (15)	31 (15)	27 (5)	24 (5)	NA
Ferritin (μg/L) [20–250]	415 (758)	381 (303)	306 (199)	342 (411)	31 (-)
HS diagnotics					
EMA (%)	87 (13)	75 (9)	72 (8)	74 (8)	88 (-)

Mean values are presented (±standard deviation). Mean values in hemoglobin ($p < 0.05$), absolute reticulocyte count ($p < 0.01$) and EMA ($p < 0.05$) differed significantly between the categories displayed in bright and light orange. EMA = eosin-5-maleimide binding test; NA = no available data.

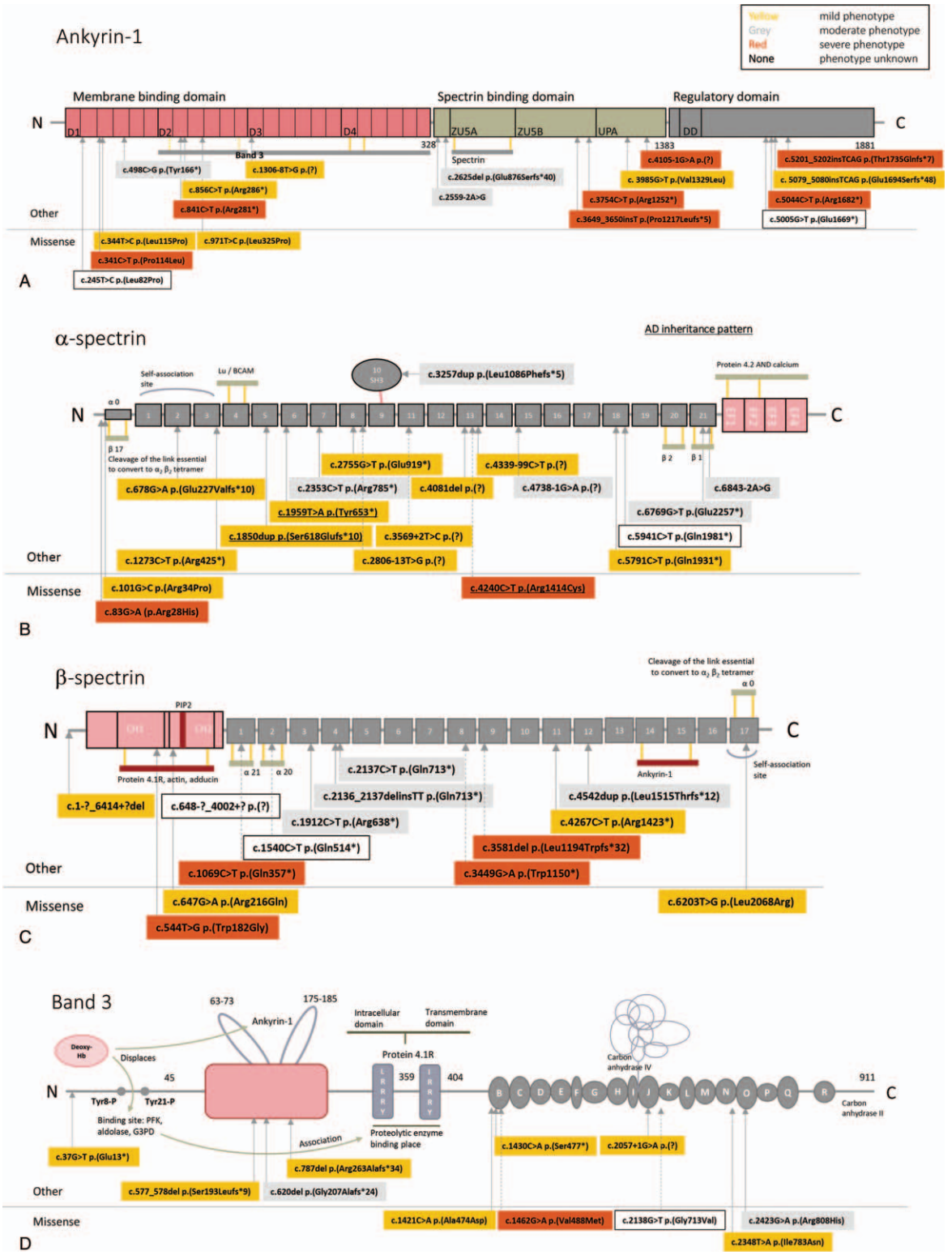

Figure 2. All pathogenic mutations were mapped along the protein structures of ankyrin-1, α-spectrin, β-spectrin and band 3. Mutations were colored by phenotype. All mutations in *ANK1, SCL4A1,* and *SPTB* were inherited following an AD pattern. Of the novel mutations in the *SPTA1* gene, 3 mutations were inherited in an AD fashion. Information on coinheritance of the modifying α^{LELY} mutation is provided in *table 2*. Panel A. Ankyrin.[3,55,56] The membrane domain consists of 24 ankyrin repeats grouped per 6 repeats. The membrane domain harbors 2 binding sites for Band 3. The spectrin domain consists of 3 subdomains, ZU5A contains the binding site for spectrin. The regulatory domain might modulate binding properties of the other domains. The function of the death domain (DD) is currently unknown. Panel B&C. A- and β-spectrin.[3,55,57] The membrane protein spectrin is composed of 2 chains, α- and β-spectrin. Both spectrin chains contain a number of spectrin-type repeats with specialized domains for self-association, spectrin, ankyrin-1 (head), actin, protein 4.1R and other proteins (tail) binding. Panel D. Band 3.[3,55,58–60] The protein consists of an intracellular (*N-terminus)* and a transmembrane domain (*C-terminus*). The intracellular domain forms the attachment site for the components of the membrane cytoskeleton, glycolytic enzymes. Deoxyhemoglobin or phosphorylation of Tyr21 or Tyr8 displaces, and thereby activates, PFK, aldolase and G3PD. Deoxyhemoglobin might also displace ankyrin-1. Ankyrin-1 and protein 4.1R inhibit each other's binding to band 3. The transmembrane domain forms an anion-exchange channel.

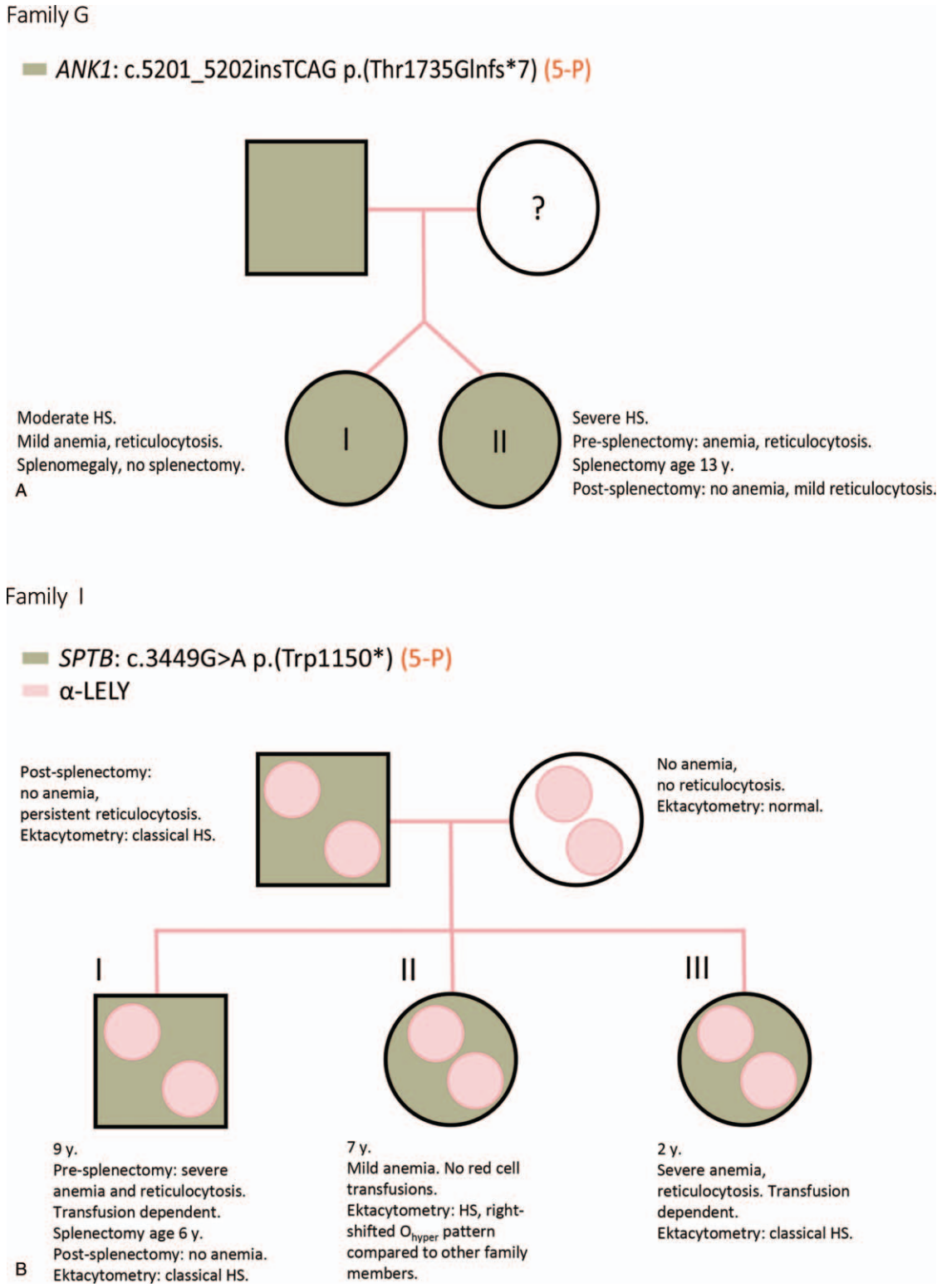

Figure 3. Overview of genetic mutations and phenotypes in 2 families with HS (family G and I). Panel A. Pathogenic *ANK1* mutation, c.5201_5202insTCAG p.(Thr1735Glnfs*7) (5-P) in dizygotic twins. Patient I had a moderate phenotype with mild anemia (Hb 10.5–12 g/dL), reticulocytosis (15–20%) and mild splenomegaly. Patient II had a severe phenotype (Hb 8.0–10.0 g/dL; reticulocytosis ±20%), ultimately leading to splenectomy at the age of 13y. Panel B. Pathogenic *SPTB* mutation, c.3449G>A p.(Trp1150*) (5-P) in father and 3 siblings. Father, and sibling I and III had a severe phenotype with transfusion-dependency and the need for splenectomy. Sibling II had a milder phenotype with a remarkably different pattern of the Osmoscan curve with a right-shifted Ohyper.

with mutations in the domains for spectrin dimer-tetramer association and ankyrin-spectrin-binding domains of ankyrin-1, α-spectrin and β-spectrin. Earlier research in mice with severe HS due to different homozygous *SPTA1* mutations, showed that the expression of various proteins of the ankyrin complex varied. Interestingly, a missense mutation in the highly conserved

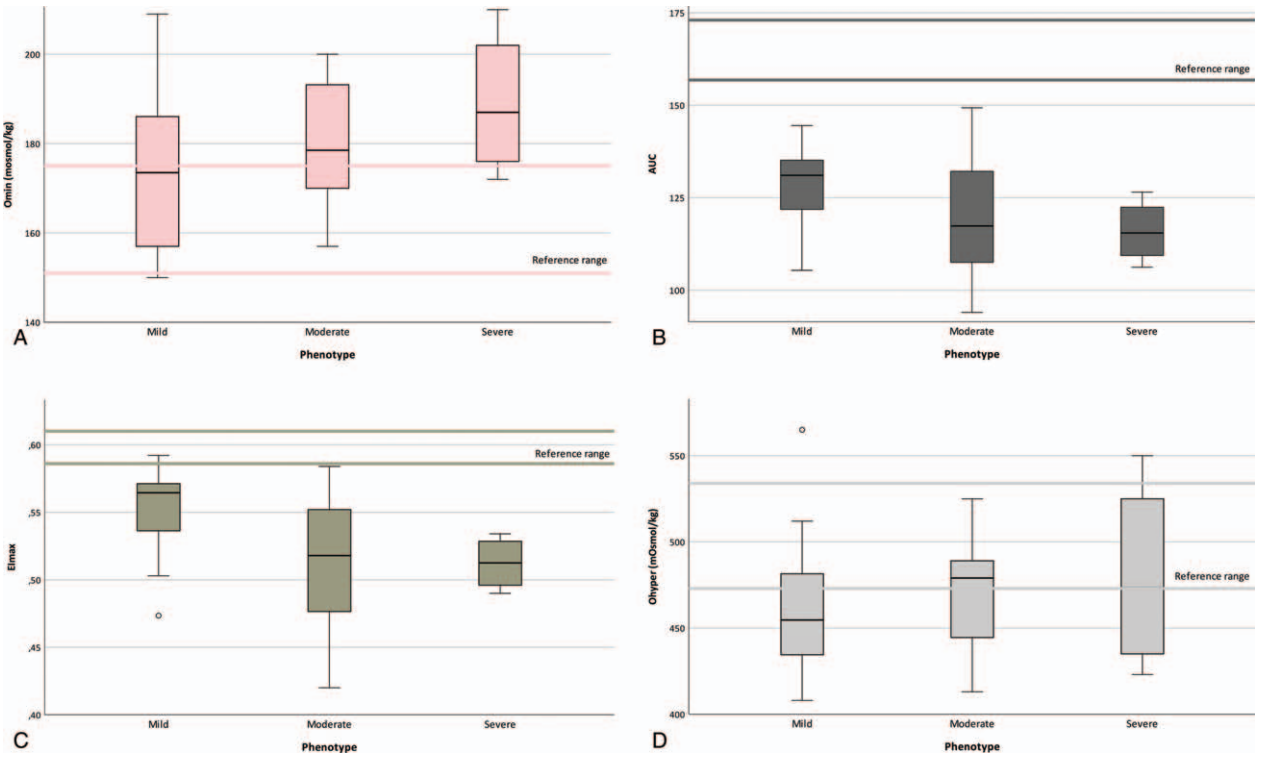

Figure 4. Omin, Ohyper, Elmax and Area Under the Curve (LoRRca, Maxsis) and their relation to HS phenotype. The graphs show box plots with median value, first and third quartile and minimum and maximum values. Omin (panel A), AUC (Panel B), Elmax (panel C) and Ohyper (panel D) values are visualized for a group of 44 HS patients (mild N = 28, moderate N = 12, severe N = 4). The reference range is depicted by 2 colored lines (upper and lower limit). Values are organized by HS phenotype (mild, moderate or severe). The AUC was below the reference limit in all patients; Elmax was below the reference range in 43/44 patients; Ohyper was below the reference range in 24/44 patients; and 23/44 had an Omin value above the reference range.

cysteine residue at the C-terminus of *SPTA1*, resulted in near-normal amounts of spectrin, band 3 and β-adducin, but still in an severe HS phenotype, due to disruption of a critical interaction domain for membrane stability.[30] Based on these findings, we suggest that determining expression of the distinct membrane proteins may increase our insights in RBC static skeletal conformation.[24]

At the same time, RBC deformability measurements reflect dynamic properties of the assembled membrane.[18,19] To further investigate the genotype-phenotype correlation, we therefore evaluated functional RBC parameters and cellular dynamics. We previously demonstrated in 21 HS patients that, regardless of the genotype, RBC density, intercellular heterogeneity and deformability were strong markers of clinical disease severity.[31] In line with these latter observations, we here demonstrate that various parameters displaying RBC deformability in osmotic gradient conditions, EImax, AUC and Omin, were significantly associated with disease severity. Omin correspondents to the 50% lysis point determined by the classical osmotic fragility test.[32,33] The lack of an association between disease severity and Ohyper values might be explained by the observation of 2 distinct Osmoscan profiles in HS patients: a classical profile with low Ohyper values, and a right-shifted 1 with relatively high Ohyper values.[34] The cause and relevance of this right-shifted profile remains to be established.

In contrast with our findings, Zaninoni et al[34] recently reported the absence of an association between the severity of anemia and Osmoscan parameters in their cohort of 116 HS patients. There were important differences in the assembly of both cohorts: the cohort of Zaninoni et al[34] consisted of splenectomized and non-splenectomized patients, which likely have influenced hemoglobin concentrations. Here, we conclude that functional RBC deformability parameters (EImax and AUC) are clearly associated with HS phenotype.

We detected various mutation types in our HS cohort that we categorized as missense and non-missense mutations. It was previously suggested that non-missense mutations would mainly result in the introduction of premature stopcodons, thereby leading to either expression of truncated protein or to nonsense-mediated-decay of the resulting mRNA and a lack of expression from the concerning allele, rather than affecting protein function.[3] While this seems to suggest that non-missense mutations induce largely comparable phenotypes, our data does not support this suggestion. In addition, it has previously been shown that non-missense mutations leading to a premature stop codon in the spectrin-binding domain of ankyrin resulted in a more severe phenotype than similar mutations in one of the other functional domains of the ankyrin protein.[29] In our cohort, we observed that β-spectrin deficiency due to deletion of one *SPTB* allele, resulted in phenotypically milder HS compared to most of the other *SPTB* mutations, missense and non-missense. Thereby, our data is suggestive of incorporation of truncated protein which disrupts cytoskeleton function and is thereby more harmful than reduction in the amount of normally formed protein.

Phenotypic heterogeneity in patients with identical pathogenic HS mutations can be the result of the effects of concomitant mutations in modifier genes, including the low-expression alleles of *SPTA1* α^{LEPRA} and α^{LELY}.[35–37] In our study, we were not able to explain phenotypic heterogeneity in family studies based on known genetic modifiers. Yet-unknown genetic factors might

play a role in the observed phenotypic variability. It could even involve non-genetic factors that might influence the amount of protein, or might disrupt its interactions in the RBC cytoskeleton. With regard to the genetic factors, current research in our laboratory focuses on 88 additional genes hypothetically involved in RBC (membrane) disorders based on their functional role and/or the association with hemolytic anemia in animal models. Over the last years unbiased genetic testing, including whole exome sequencing,[38–40] identified new genes involved in hereditary anemias; thereby expanding the targeted-NGS panels for congenital RBC disorders from a few genes to large panels.[23,41–46] Expanding these panels with, for example, genes associated with hyporegenerative anemias, defective erythropoiesis, and metabolic defects allows identification of cases in which phenotypic variability could be explained by coinheritance of multiple RBC diseases.[23,41,42]

We are the first to report 3 novel *SPTA1* mutations with an apparent AD inheritance pattern. Theoretically this can be explained by distinct underlying pathophysiological mechanisms. First, there might have been co-inheritance of yet-unknown modifying mutations that have influenced α-spectrin expression or its interactions. Second, a *SPTA1* null-allele will become clinically relevant, as α-spectrin becomes the rate-determining component of α/β-heterodimer assembly. Under physiologic conditions there is an overproduction of α- compared to β-spectrin (ratio 3:1).[35,47] Changes in the α-/β-spectrin ratio towards a 1:1 ratio were observed in band 3 deficient membranes,[48] and after erythropoietin stimulation under anemic conditions.[49] Third, we assume that current high rate of screening laboratory assessments plays a role, leading to the diagnosis of very mild, asymptomatic forms of HS resulting from an heterozygous *SPTA1* mutation. Future studies will be necessary to provide insight in those factors resulting in clinically relevant HS in case of one mutated *SPTA1* allele.

In conclusion, our data underline that the genotype-phenotype correlation in HS is highly complex due to the complexity of the interactions in the RBC cytoskeleton. The pathogenic mutation, amount and quality of incorporated protein, effects of truncated protein or its absence on the interactions in the cytoskeleton determine clinical disease severity. Thereby, presence of modifying genetic and even non-genetic factors influences phenotypic variability. Based on our findings, we conclude that knowledge of underlying molecular defects as well as functional analysis of RBC deformability are required to understand phenotypic variability in HS.

Materials and methods

Data source and study population

We retrospectively included patients diagnosed with HS based on analyses performed in the period from January 2014 through January 2018. Patients diagnosed with HS were selected from all patients referred to the tertiary expertise center for rare anemia in the Netherlands (University Medical Center Utrecht, Utrecht, The Netherlands), based on a clinical suspicion of hemolytic anemia due to HS. According to the ICSH (International Council for Standardization in Hematology) guidelines for laboratory diagnosis of nonimmune hereditary RBC membrane disorders,[50] diagnosis of HS was based on a composite of currently available tests including EMA, osmotic fragility test and osmotic gradient ektacytometry (Osmoscan), combined with hematologic and laboratory markers of hemolysis, clinical data, family history and morphological analysis of peripheral blood samples.

Next-generation sequencing

Sequence analysis was conducted in the ISO15189 accredited genome diagnostics laboratory of the UMC Utrecht. In short: Genomic DNA was isolated from peripheral blood samples of the patients and enriched for, among others, 7 genes associated with HS (*SPTA1, SPTB, ANK1, SLC4A1, EPB41, EPB42, RHAG*) using a custom designed Agilent SureSelect^{XT} capture library (ELID#:0497291) or the SureSelect^{XT} Clinical Research Exome V2 (ELID#:30409818). NGS samples were sequenced to a minimum average depth of 100X on either a Life-Technologies/Applied Biosystems SOLiD^{TM} 5500XL Sequencer (50 bp single reads), an Illumina HiSeq2500 Sequencer (2x100 bp paired end reads) or an Illumina Novaseq6000 Sequencer (2x 150 bp paired end reads). Horizontal coverage (the average number of reads that align to the known reference bases) of the 7 HS-associated genes analyzed in the gene panel hereditary spherocytosis was at least 99% with >15 unique reads per base for all sequencers. Raw sequence reads were mapped to the hg19 human genome reference, and variations were called using a in house developed bioinformatics pipeline. Variants were subsequently annotated and classified in the Alissa Interpret software suite (Agilent Technologies) using a custom build, ISO15189 validated, variant classification tree, adhering to the American College of Medical Genetics and Genomics Standards and guidelines for the interpretation of sequence variants.[28] Clinically relevant mutations were confirmed by Sanger sequencing.

Laser assisted optical rotational cell analyzer

Osmotic gradient ektacytometry using the Osmoscan module on the LoRRca MaxSis (RR Mechatronics, Zwaag, The Netherlands) measures RBC deformability, expressed as Elongation Index (EI), during constant shear stress as a function of continuously changing osmotic conditions. Deformability depends on the total membrane surface area, surface area to volume ratio, and cellular hydration status. In RBC, membrane disorders these features are generally altered.[18,19] For osmotic gradient ektacytometry measurements of RBCs from HS patients 250 μL of whole blood was standardized to a hemoglobin concentration of 12.9 g/dL and injected in 5 mL isotonic polyvinylpyrrolidone (PVP), and osmotic gradient ektacytometry was further carried out as previously described.

Four parameters of the Osmoscan curve are diagnostically relevant: EImax, Omin, Ohyper, and the AUC. These reflect mean surface area (EImax), surface to volume ratio (Omin), and cellular hydration status (Ohyper). The typical Osmoscan curve in HS patients is characterized by a decreased EImax, an elevated Omin value (shift to the right) and decreased Ohyper value (shift to the left), and consequently a decrease in AUC.[34]

Study conduct and data analysis

The study was conducted according to Good Clinical Practice guidelines, defined by the International Conference on Harmonisation (ICH). Mutations were categorized based on affected gene, type of mutation (missense versus other, including nonsense, frameshift, indels or splicesite mutation) and co-inheritance of low expression polymorphisms (eg, Spα^{LELY} or

Spα^{LEPRA}). Hematologic parameters were provided by the referring institutes. Per patient the mean values of the hematologic and hemolysis parameters from samples obtained during the year before and after genetic analysis were included. If only one assessment was available during this time frame, a second assessment obtained less than 5 years from genetic analysis was included. In those cases, in which splenectomy was performed mean values obtained 2 years before and/or after splenectomy were reported. In infants, hematologic parameters obtained before the age of 1 year were not included in the final analyses based on distinct reference values in the first year of life. Due to the existence of inter-institution variance in absolute reticulocyte counts, only reticulocyte counts measured in our own institute were included. Information about the inheritance patterns was provided by the referring hematologist.

Statistical analysis

To explore phenotypic variability patients were categorized based on the underlying genetic defect. Differences between groups were tested with one-way Analysis of Variance (ANOVA), followed by Tukey's HSD post-hoc test. Correlation analyses of hematologic parameters and genetic subgroups were reported using Pearson's correlation coefficient. To correct for potential bias *bootstrapping* was performed to confirm significance.[51,52] The association between Osmoscan curve parameters and disease severity was tested using Spearman's rank correlation test. Statistical significance was set at a 2-sided $p < 0.05$. All calculations were performed using IBM SPSS Statistics v. 25.

References

1. Mohandas N, Gallagher PG. Red cell membrane: Past, present, and future. *Blood.* 2008;112:3939–3948. doi: 10.1182/blood-2008-07-161166 [doi].
2. Pesciotta EN, Sriswasdi S, Tang HY, et al. A label-free proteome analysis strategy for identifying quantitative changes in erythrocyte membranes induced by red cell disorders. *J Proteomics.* 2012;(76 Spec No.):194–202. doi: 10.1016/j.jprot.2012.08.010 [doi].
3. Lux SE. Anatomy of the red cell membrane skeleton: Unanswered questions. *Blood.* 2016;127:187–199. doi: 10.1182/blood-2014-12-512772 [doi].
4. Mohandas N, Evans E. Mechanical properties of the red cell membrane in relation to molecular structure and genetic defects. *Annu Rev Biophys Biomol Struct.* 1994;23:787–818. doi: 10.1146/annurev.bb.23.060194.004035 [doi].
5. Narla J, Mohandas N. Red cell membrane disorders. *Int J Lab Hematol.* 2017;39 (Suppl 1):47–52. doi: 10.1111/ijlh.12657 [doi].
6. Perrotta S, Gallagher PG, Mohandas N. Hereditary spherocytosis. *Lancet.* 2008;372:1411–1426. doi: 10.1016/S0140-6736(08)61588-3 [doi].
7. Reliene R, Mariani M, Zanella A, et al. Splenectomy prolongs in vivo survival of erythrocytes differently in spectrin/ankyrin- and band 3-deficient hereditary spherocytosis. *Blood.* 2002;100:2208–2215.
8. Safeukui I, Buffet PA, Deplaine G, et al. Quantitative assessment of sensing and sequestration of spherocytic erythrocytes by the human spleen. *Blood.* 2012;120:424–430. doi: 10.1182/blood-2012-01-404103 [doi].
9. Gallagher PG. Abnormalities of the erythrocyte membrane. *Pediatr Clin North Am.* 2013;60:1349–1362. doi: 10.1016/j.pcl.2013.09.001 [doi].
10. Da Costa L, Galimand J, Fenneteau O, et al. Hereditary spherocytosis, elliptocytosis, and other red cell membrane disorders. *Blood Rev.* 2013;27:167–178. doi: 10.1016/j.blre.2013.04.003 [doi].
11. Cynober T, Mohandas N, Tchernia G. Red cell abnormalities in hereditary spherocytosis: Relevance to diagnosis and understanding of the variable expression of clinical severity. *J Lab Clin Med.* 1996;128:259–269. doi: S0022-2143(96)90027-X [pii].
12. Jandl JH, Simmons RL, Castle WB. Red cell filtration and the pathogenesis of certain hemolytic anemias. *Blood.* 1961;18:133–148.
13. He BJ, Liao L, Deng ZF, et al. Molecular genetic mechanisms of hereditary spherocytosis: current perspectives. *Acta Haematol.* 2018;139:60–66. doi: 10.1159/000486229 [doi].
14. Van Wijk R, Vogel M, Elferink M, et al. Next generation sequencing in the diagnosis of red cell membrane disorders. *Int J Lab Hematol.* 2014;36 ((Suppl. 1)): Abstract O45.
15. van Dijk EL, Jaszczyszyn Y, Naquin D, et al. The third revolution in sequencing technology. *Trends Genet.* 2018;34:666–681. doi: S0168-9525(18)30096-9 [pii].
16. Agarwal AM, Nussenzveig RH, Reading NS, et al. Clinical utility of next-generation sequencing in the diagnosis of hereditary haemolytic anaemias. *Br J Haematol.* 2016;174:806–814. doi: 10.1111/bjh.14131 [doi].
17. King MJ, Zanella A. Hereditary red cell membrane disorders and laboratory diagnostic testing. *Int J Lab Hematol.* 2013;35:237–243. doi: 10.1111/ijlh.12070 [doi].
18. Da Costa L, Suner L, Galimand J, et al. Diagnostic tool for red blood cell membrane disorders: Assessment of a new generation ektacytometer. *Blood Cells Mol Dis.* 2016;56:9–22. doi: 10.1016/j.bcmd.2015.09.001 [doi].
19. Lazarova E, Gulbis B, Oirschot BV, et al. Next-generation osmotic gradient ektacytometry for the diagnosis of hereditary spherocytosis: Interlaboratory method validation and experience. *Clin Chem Lab Med.* 2017;55:394–402. doi: 10.1515/cclm-2016-0290 [doi].
20. Eber SW, Gonzalez JM, Lux ML, et al. Ankyrin-1 mutations are a major cause of dominant and recessive hereditary spherocytosis. *Nat Genet.* 1996;13:214–218. doi: 10.1038/ng0696-214 [doi].
21. Yawata Y, Kanzaki A, Yawata A, et al. Characteristic features of the genotype and phenotype of hereditary spherocytosis in the japanese population. *Int J Hematol.* 2000;71:118–135.
22. Iolascon A, Avvisati RA. Genotype/phenotype correlation in hereditary spherocytosis. *Haematologica.* 2008;93:1283–1288. doi: 10.3324/haematol.13344 [doi].
23. He Y, Jia S, Dewan RK, et al. Novel mutations in patients with hereditary red blood cell membrane disorders using next-generation sequencing. *Gene.* 2017;627:556–562. doi: S0378-1119(17)30521-8 [pii].
24. Mariani M, Barcellini W, Vercellati C, et al. Clinical and hematologic features of 300 patients affected by hereditary spherocytosis grouped according to the type of the membrane protein defect. *Haematologica.* 2008;93:1310–1317. doi: 10.3324/haematol.12546 [doi].
25. Pugi J, Drury LJ, Langer JC, et al. Genotype/phenotype correlations in 103 children from 87 families with hereditary spherocytosis. *Blood.* 2016;128:2432.
26. Iolascon A, Andolfo I, Barcellini W, et al. Recommendations regarding splenectomy in hereditary hemolytic anemias. *Haematologica.* 2017;102:1304–1313. doi: 10.3324/haematol.2016.161166 [doi].
27. Eber SW, Armbrust R, Schroter W. Variable clinical severity of hereditary spherocytosis: Relation to erythrocytic spectrin concentration, osmotic fragility, and autohemolysis. *J Pediatr.* 1990;117:409–416.
28. Richards S, Aziz N, Bale S, et al. Standards and guidelines for the interpretation of sequence variants: A joint consensus recommendation of the american college of medical genetics and genomics and the association for molecular pathology. *Genet Med.* 2015;17:405–424. doi: 10.1038/gim.2015.30 [doi].
29. Park J, Jeong DC, Yoo J, et al. Mutational characteristics of ANK1 and SPTB genes in hereditary spherocytosis. *Clin Genet.* 2016;90:69–78. doi: 10.1111/cge.12749 [doi].
30. Robledo RF, Lambert AJ, Birkenmeier CS, et al. Analysis of novel sph (spherocytosis) alleles in mice reveals allele-specific loss of band 3 and adducin in alpha-spectrin-deficient red cells. *Blood.* 2010;115:1804–1814. doi: 10.1182/blood-2009-07-232199 [doi].
31. Huisjes R, Makhro A, Llaudet-Planas E, et al. Density, heterogeneity and deformability of red cells as markers of clinical severity in hereditary spherocytosis. *Hemasphere.* 2018;2 (S1):513.
32. Clark MR, Mohandas N, Shohet SB. Osmotic gradient ektacytometry: Comprehensive characterization of red cell volume and surface maintenance. *Blood.* 1983;61:899–910.
33. Huisjes R, Bogdanova A, van Solinge WW, et al. Squeezing for life - properties of red blood cell deformability. *Front Physiol.* 2018;9:656doi: 10.3389/fphys.2018.00656 [doi].
34. Zaninoni A, Fermo E, Vercellati C, et al. Use of laser assisted optical rotational cell analyzer (LoRRca MaxSis) in the diagnosis of RBC membrane disorders, enzyme defects, and congenital dyserythropoietic anemias: A monocentric study on 202 patients. *Front Physiol.* 2018;9:451doi: 10.3389/fphys.2018.00451 [doi].

35. Delaunay J, Nouyrigat V, Proust A, et al. Different impacts of alleles alphaLEPRA and alphaLELY as assessed versus a novel, virtually null allele of the SPTA1 gene in trans. *Br J Haematol.* 2004;127:118–122. doi: 10.1111/j.1365-2141.2004.05160.x [doi].
36. Wichterle H, Hanspal M, Palek J, et al. Combination of two mutant alpha spectrin alleles underlies a severe spherocytic hemolytic anemia. *J Clin Invest.* 1996;98:2300–2307. doi: 10.1172/JCI119041 [doi].
37. Wilmotte R, Harper SL, Ursitti JA, et al. The exon 46-encoded sequence is essential for stability of human erythroid alpha-spectrin and heterodimer formation. *Blood.* 1997;90:4188–4196.
38. Boycott KM, Vanstone MR, Bulman DE, et al. Rare-disease genetics in the era of next-generation sequencing: Discovery to translation. *Nat Rev Genet.* 2013;14:681–691. doi: 10.1038/nrg3555 [doi].
39. Katsanis SH, Katsanis N. Molecular genetic testing and the future of clinical genomics. *Nat Rev Genet.* 2013;14:415–426. doi: 10.1038/nrg3493 [doi].
40. Rehm HL. Disease-targeted sequencing: A cornerstone in the clinic. *Nat Rev Genet.* 2013;14:295–300. doi: 10.1038/nrg3463 [doi].
41. Russo R, Andolfo I, Manna F, et al. Multi-gene panel testing improves diagnosis and management of patients with hereditary anemias. *Am J Hematol.* 2018;93:672–682. doi: 10.1002/ajh.25058 [doi].
42. Andolfo I, Russo R, Gambale A, et al. New insights on hereditary erythrocyte membrane defects. *Haematologica.* 2016;101:1284–1294. doi: haematol.2016.142463 [pii].
43. Andolfo I, Alper SL, De Franceschi L, et al. Multiple clinical forms of dehydrated hereditary stomatocytosis arise from mutations in PIEZO1. *Blood.* 2013;121:3925–3935. doi: 10.1182/blood-2013-02-482489 [doi].
44. Andolfo I, Russo R, Manna F, et al. Novel gardos channel mutations linked to dehydrated hereditary stomatocytosis (xerocytosis). *Am J Hematol.* 2015;90:921–926. doi: 10.1002/ajh.24117 [doi].
45. Albuisson J, Murthy SE, Bandell M, et al. Dehydrated hereditary stomatocytosis linked to gain-of-function mutations in mechanically activated PIEZO1 ion channels. *Nat Commun.* 2013;4:1884doi: 10.1038/ncomms2899 [doi].
46. Andolfo I, Alper SL, Delaunay J, et al. Missense mutations in the ABCB6 transporter cause dominant familial pseudohyperkalemia. *Am J Hematol.* 2013;88:66–72. doi: 10.1002/ajh.23357 [doi].
47. Hanspal M, Palek J. Synthesis and assembly of membrane skeletal proteins in mammalian red cell precursors. *J Cell Biol.* 1987;105:1417–1424.
48. Peters LL, Shivdasani RA, Liu SC, et al. Anion exchanger 1 (band 3) is required to prevent erythrocyte membrane surface loss but not to form the membrane skeleton. *Cell.* 1996;86:917–927. doi: S0092-8674(00)80167-1 [pii].
49. Hanspal M, Kalraiya R, Hanspal J, et al. Erythropoietin enhances the assembly of alpha,beta spectrin heterodimers on the murine erythroblast membranes by increasing beta spectrin synthesis. *J Biol Chem.* 1991;266:15626–15630.
50. King MJ, Garcon L, Hoyer JD, et al. ICSH guidelines for the laboratory diagnosis of nonimmune hereditary red cell membrane disorders. *Int J Lab Hematol.* 2015;37:304–325. doi: 10.1111/ijlh.12335 [doi].
51. Bland JM, Altman DG. Statistics notes: Bootstrap resampling methods. *BMJ.* 2015;350:h2622doi: 10.1136/bmj.h2622 [doi].
52. Curran-Everett D. Explorations in statistics: The assumption of normality. *Adv Physiol Educ.* 2017;41:449–453. doi: 10.1152/advan.00064.2017 [doi].
53. den Dunnen JT, Dalgleish R, Maglott DR, et al. HGVS recommendations for the description of sequence variants: 2016 update. *Hum Mutat.* 2016;37:564–569. doi: 10.1002/humu.22981 [doi].
54. Marechal J, Wilmotte R, Kanzaki A, et al. Ethnic distribution of allele alpha LELY, a low-expression allele of red-cell spectrin alpha-gene. *Br J Haematol.* 1995;90:553–556.
55. ClinVar database, https://Www.ncbi.nlm.nih.gov/clinvar/. 2018.
56. Yasunaga M, Ipsaro JJ, Mondragon A. Structurally similar but functionally diverse ZU5 domains in human erythrocyte ankyrin. *J Mol Biol.* 2012;417:336–350. doi: 10.1016/j.jmb.2012.01.041 [doi].
57. Li X, Bennett V. Identification of the spectrin subunit and domains required for formation of spectrin/adducin/actin complexes. *J Biol Chem.* 1996;271:15695–15702.
58. Barneaud-Rocca D, Etchebest C, Guizouarn H. Structural model of the anion exchanger 1 (SLC4A1) and identification of transmembrane segments forming the transport site. *J Biol Chem.* 2013;288:26372–26384. doi: 10.1074/jbc.M113.465989 [doi].
59. Ding Y, Casey JR, Kopito RR. The major kidney AE1 isoform does not bind ankyrin (Ank1) in vitro. an essential role for the 79 NH2-terminal amino acid residues of band 3. *J Biol Chem.* 1994;269:32201–32208.
60. Satchwell TJ, Hawley BR, Bell AJ, et al. The cytoskeletal binding domain of band 3 is required for multiprotein complex formation and retention during erythropoiesis. *Haematologica.* 2015;100:133–142. doi: 10.3324/haematol.2014.114538 [doi].